

MIT Open Access Articles

“Batch” Kinetics in Flow: Online IR Analysis and Continuous Control

The MIT Faculty has made this article openly available. **Please share** how this access benefits you. Your story matters.

Citation: Moore, Jason S., and Klavs F. Jensen. “‘Batch’ Kinetics in Flow: Online IR Analysis and Continuous Control.” *Angewandte Chemie International Edition* 53, no. 2 (November 29, 2013): 470–473.

As Published: <http://dx.doi.org/10.1002/anie.201306468>

Publisher: Wiley Blackwell

Persistent URL: <http://hdl.handle.net/1721.1/92777>

Version: Original manuscript: author's manuscript prior to formal peer review

Terms of use: Creative Commons Attribution-Noncommercial-Share Alike



“Batch” Kinetics in Flow with Online IR Analysis and Continuous Control**

Jason S. Moore and Klavs F. Jensen*

Current methods for generating kinetic data can be categorized as either sampling steady-state conditions in flow or generating time-series data in batch.^[1] The latter method has proven particularly useful in identifying complex kinetic mechanisms.^[2] Unfortunately, both of these techniques have significant limitations. While continuous flow experiments, especially in microreactors, have advantages over batch in terms of mixing times,^[3,4] temperature control,^[5,6] materials savings,^[7] and the ability to perform sequential experiments without intermediate cleaning steps, batch experiments are seen as better suited to generating kinetic data due to the ability to collect data from many time points in a single experiment.^[2] However, with continuous online measurement, flow experiments can generate such time-series data by continuously varying flow rate in a low-dispersion reactor.^[8] This analysis is possible because, under ideal conditions, a batch reactor and a plug-flow reactor have the same kinetics design equation; *i.e.*, they will have the exact same conversion as a function of conditions and time for any reaction, as time in the batch reactor corresponds to residence time in the plug flow reactor.^[1] These reactors are typically treated differently only due to deviations from ideality, such as concentration or temperature gradients from imperfect mixing.

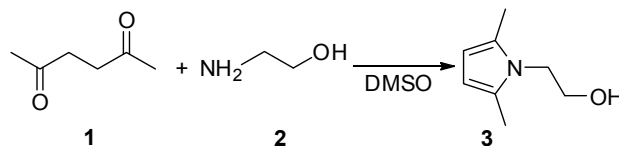
A recent contribution by Mozharov *et al.* presented a method to take advantage of the ideality of microreactors to derive time-series data *via* flow manipulation.^[9] In their method, a Knoevenagel condensation in a microreactor was allowed to come to steady state at a low flow rate. A step change in flow rate then rapidly flushed the contents of the reactor. As this reactor volume exited, an inline Raman probe measured the product concentration. While this enabled generation of a conversion curve in agreement with steady-state experiments, the exact reaction times during this flow-rate step change could not be known because the step change was not actually instantaneous, requiring graphical and empirical estimation of reaction times. As stated in Mozharov *et al.*, “The step increase in flow rate is never perfect. The system always needs some time to speed up to the higher flow rate... The exact function $F(\tau)$ during this transitional period is uncertain.”^[9] This non-ideality is due to effects such as non-rigidity of tubing walls and the syringe plunger,

preventing an immediate change in the pressure profile throughout the system.

The method developed here involves allowing a microreactor system to come to steady state at short residence time, which significantly reduces the initial waiting period before flow manipulation can begin. Uncertainty in accurate determination of residence time is avoided through a controlled ramp rather than a step change in flow rate. This enables the rate of the change in residence time to be set, allowing control over the trade-off between more experimental data and experiment duration.

This work focuses on describing this new methodology and is intended to be broadly applicable to a wide range of chemistries for which time-series data are desired. Ideally, this method could be applied with inline analysis to any chemistry capable of being quenched chemically, thermally, or otherwise. However, an integrated online sensor at the end of the reaction zone would allow this method to be expanded even further. As such, ATR-FTIR, UV/Vis, flow NMR, Raman, fluorescence spectrometry, and more are amenable to this technique.

The efficacy of this new technique was demonstrated using a Paal-Knorr reaction of 2,5-hexanedione (1) and ethanolamine (2) in dimethyl sulfoxide (DMSO) (Schemes 1 and 2)^[10,11] in an automated flow platform (Figure S1),^[12,13] which used an inline Mettler Toledo ReactIR ATR-FTIR flow cell^[14] to continuously monitor the effluent from a silicon microreactor.



Scheme 1. Paal-Knorr reaction.^[15,16]

[*] Jason S. Moore, Prof. Klavs F. Jensen
Department of Chemical Engineering
Massachusetts Institute of Technology
77 Massachusetts Avenue, 66-342, Cambridge, MA 02139
(USA)
Fax: (+1) 617-258-8992
E-mail: k Jensen@mit.edu
Homepage: <http://web.mit.edu/jensenlab>

Jason S. Moore
The Dow Chemical Company
2301 North Brazosport Blvd., B-1603, Freeport, TX 77541
(USA)

[**] We thank Novartis for financial support.

Supporting information for this article is available on the WWW under <http://www.angewandte.org>.

Scheme 2. Paal-Knorr reaction mechanism.^[11,17,18]

For the microreactor system used, the narrow channel widths (400 μm) allow diffusion to rapidly eliminate radial concentration gradients, leading to minimal dispersion for the conditions tested.^[1,8] Under such conditions of low dispersion, a flow reactor may be

treated as a series of batch reactors (Figure 1). This treatment allows well-controlled system transients to be used to generate kinetic information much more rapidly than with traditional flow experiments, requiring only that the history of each fluid element is known when it exits the reactor.

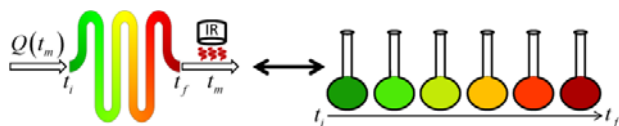


Figure 1. Treatment of a low-dispersion flow reactor as a series of well-mixed batch reactors. Color represents extent of conversion from low (green) to high (red).

The method used to generate this time profile is to set the flow rate initially to give a short residence time, τ_0 , in the system of volume V_r . After this system has reached steady state, the residence time is gradually increased at a constant rate, α , times the experiment time, t , by reducing the flow rate, Q , in a controlled manner such that the system instantaneous residence time, τ_{ins} , is always known.

$$\tau_{ins} = \tau_0 + \alpha t = \frac{V_r}{Q(t)} \quad (1)$$

Each “pseudo-batch” reactor passes through the reactor in a time τ from initial time, t_i , to final time, t_f , which are unique for each fluid element. The residence time each fluid element spends in the reactor is a function of when it exits the reactor,

$$\tau = t_f - t_i = \left(1 - e^{-\alpha}\right) \left(t_f + \frac{\tau_0}{\alpha}\right) \quad (2)$$

This expression can be rewritten as the linear residence time ramp

$$\tau = \frac{S}{\alpha} \tau_0 + S t_f \quad (3)$$

where S is the slope of τ versus t_f :

$$S = \left(1 - e^{-\alpha}\right) \quad (4)$$

An example of the resulting residence time profile is given in Figure S2, along with additional derivations. This method results in a predictable and accurate residence time profile. Furthermore, the reactor effluent can be measured for a longer period to reduce variability and increase data collection. This approach enables a greater sampling rate of the experimentally collected conversion data (Figure S3) with a data density 10-fold higher than previously reported by Mozharov *et al.*,^[9] reducing the error of estimated kinetic parameters. Coupled with a more rapid analytical technique, this method could be extended to much faster chemistries. Additionally, a lower value of S would allow the residence time to be ramped more slowly, enabling analysis at residence time intervals much closer together than the sampling frequency, further increasing the data density. Moreover, a lower value of S would also allow generation of time-series data that cannot be captured in batch systems due to reaction kinetics that result in complete conversion too quickly for conventional *in situ* analysis techniques. However, this approach would require analysis of more reactor volumes (cf. Figure S4).

A first test of the linear residence time ramp method at 130 °C with several values of S yielded residence time profile results following the same trend as the steady state values but with a slight deviation in the product concentration from the steady states that increased as S approached 1 (Figure S5). This deviation results from

the small volume between the end of the reaction zone and the inline IR flow cell due to the silicon reactor’s thermal quench zone, the reactor’s cooling block, and the tubing connecting the reactor to the IR flow cell. This delay volume, V_d , between the reactor exit and the actual measuring point is included in the model by determining the time difference between t_f , when a fluid element exits the reaction zone, and t_m , when the concentration is actually measured.

$$V_d = \int_{t_f}^{t_m} \frac{V_r}{\tau_0 + \alpha t} dt \quad (5)$$

Solving for t_m in terms of t_f gives

$$t_m = e^{\frac{V_d}{V_r} \alpha} t_f + \left(e^{\frac{V_d}{V_r} \alpha} - 1 \right) \frac{\tau_0}{\alpha} \quad (6)$$

Substituting the relationship between t_f and τ analogously to Eq. 2 gives the residence time profile as a function of t_m :

$$\tau = S e^{\frac{V_d}{V_r} \alpha} \left(t_m + \frac{\tau_0}{\alpha} \right) \quad (7)$$

Replotting the residence time profiles as a function of this residence time (Figure 2) reveals product concentrations for each residence time profile in good agreement with each other for different values of S and with the steady state concentration results.

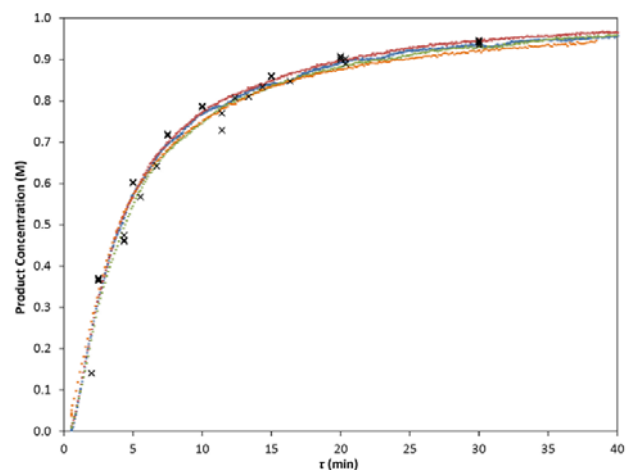


Figure 2. Residence time ramp results using corrected residence time with $S = 1/4$ (blue), $S = 1/3$ (red), $S = 1/2$ (green), and $S = 2/3$ (orange). Steady states (\times).

The method was used to generate conversion profiles at several temperatures. The data were then fit to a kinetic model (based upon Scheme 2), in which a second-order reaction, first-order in each starting material, forms an intermediate that then undergoes first-order conversion, followed by rapid conversion to the product. The reverse reaction in the first step is assumed to be significantly slower, thus having a small effect on the overall reaction rate. The automated platform was used to run multiple reaction conditions (Figure 3a). The data generated at 15 second sample intervals during the first experiment are shown in Figure 3b. These product concentration curves were then assigned to their corresponding temperatures (Figure 3c). Three experimental repeats were performed, and the two kinetic parameters, k_1 and k_2 in Scheme 2, were then fit by least-squares regression in Matlab at each temperature using every 20th data point as a test set and the rest as a

validation set. The resulting activation energies are 12.2 ± 0.4 kJ/mol and 20.0 ± 0.9 kJ/mol for reaction 1 and 2, respectively.

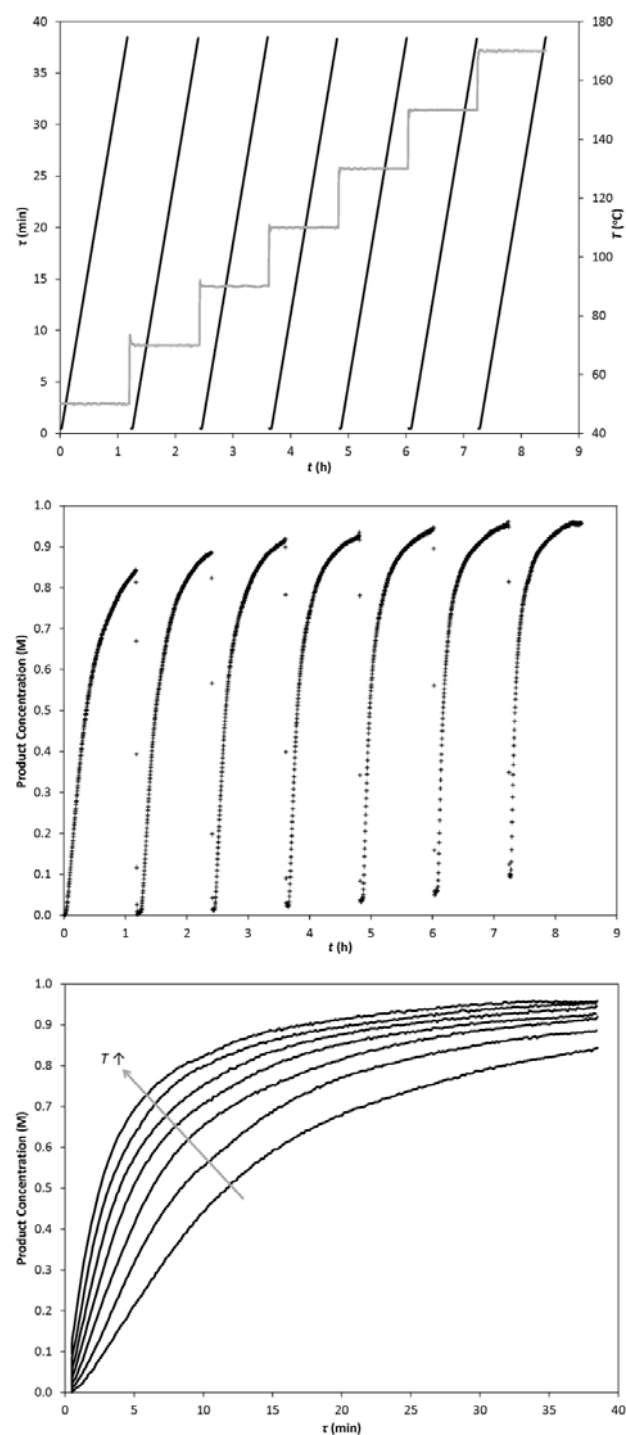


Figure 3. (a) Residence time ramps (black) and temperature steps (gray) used in the experiments. (b) Product concentration found by inline IR analysis at 15 second sample intervals. (c) Product concentration as a function of residence time at temperatures (°C) from top to bottom: 170, 150, 130, 110, 90, 70, 50.

This analysis demonstrates the significantly higher efficiency of this method to generate data for kinetic analysis over traditional

steady-state techniques. The experiment data in Figure 2 required approximately 8 hours and 5 mL of each 2 M reactant solution for completion. In contrast, had traditional steady-state reactions been performed at each temperature and residence times of 10, 20, 30, and 40 minutes, allowing four residence times for steady state,^[19-21] the experiment would have required almost 2 days and 13.5 mL of each reaction solution, and fewer data points would have been acquired.

For this example, the 15 second sample interval used in the new method allowed the collection of a large number of data points between 0.5 and 40 minutes residence time, yielding smooth conversion trends. However, as mentioned previously, even with a significantly faster reaction, the use of a value of S closer to 0 would enable significantly more data to be generated than using typical *in situ* batch techniques, allowing for elucidation of the reaction profile.

We have developed a method that rapidly generates time-series reaction data from flow reactors analogous to classical batch reaction data and in agreement with traditional steady-state flow analysis. The approach was implemented with an automated microreactor system, allowing for rapid and tight control of operating conditions. The resulting conversion-residence time profiles at several temperatures were used to fit parameters in a kinetic model, in agreement with experiments. This approach could be used to generate time-series data in flow for a wide range of chemistries. Furthermore, this method could be extended to other parameters, such as performing concentration ramps.

Experimental Section

The microfluidic system used in this work is depicted in Figure S1, including a schematic of the silicon microreactor. Two Harvard stainless steel syringes were loaded separately with 2 M solutions of 2,5-hexanedione (1) and ethanolamine (2) in dimethyl sulfoxide (DMSO), resulting in 1 M concentrations upon mixing in the reactor. One syringe was placed on each of two Harvard syringe pumps (PHD 2000) to control the residence time. The flow rates were updated each second *via* daisy-chained RS-232 communications to a Dell (Optiplex 960) computer. These syringe pumps were connected to a silicon microreactor^[22] with a 120- μ L reaction zone and a cooled inlet/outlet zone, the temperature of which was maintained at 22 °C with a recirculating VWR chiller (model 1171MD). The cooled section allowed the reactant streams to mix fully before reaction occurred and thermally quenched the reaction. The temperature of the reaction zone was controlled with an Omega (CN9311) controller and an Omega (CSH-102135/120V) heating cartridge. This controller was connected by an RS-232 cable to the computer to read the measured reactor temperature and program the temperature set point. In addition, due to the high heat transfer coefficient of silicon, the temperature of the reaction zone could be quickly changed between set points and the fluid stream rapidly reached the desired temperature in both reaction and quench zones. A Mettler Toledo ReactIR iC 10 outfitted with a DiComp ATR 10- μ L flow cell was used for continuous inline monitoring, averaging 30 spectrum scans and saving to an Excel file once every 15 seconds. Labview software (version 8.5.1) on the computer communicated with the syringe pumps and temperature controller and read the IR Excel export files to determine reaction conversion based upon calibrations to peak heights. Matlab scripts (version 2010b) within Labview controlled the reaction temperature set points and syringe pump flow rates.

For the data in Figure 3, once the temperature had equilibrated at a set point and the residence time had equilibrated at τ_0 , the residence time ramp ran for 70 minutes. The temperature set point then was changed to the next set of conditions, and the process was repeated. The duration was set at 70 minutes by adding 10 minutes to the time that would be necessary for t_f to reach 40 minutes, allowing the residence time ramp to cover nearly the full range of reaction conversions, with additional time for the reactor effluent to reach the IR flow cell.

Received: ((will be filled in by the editorial staff))

Published online on ((will be filled in by the editorial staff))

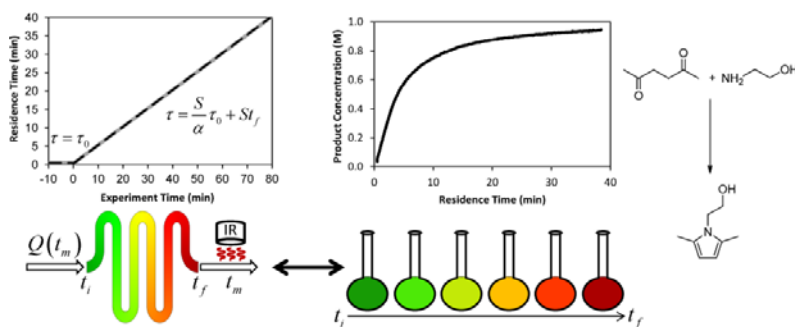
Keywords: microreactor · kinetics · automation · batch · continuous flow

-
- [1] O. Levenspiel, *Chemical Reaction Engineering*, 3rd ed.; John Wiley & Sons, 1999.
- [2] F. E. Valera, M. Quaranta, A. Moran, J. Blacker, A. Armstrong, J. T. Cabral, D. G. Blackmond, *Angew. Chem.* **2010**, *122*, 2530–2537; *Angew. Chem., Int. Ed.* **2010**, *49*, 2478–2485.
- [3] K. F. Jensen, *Chem. Eng. Sci.* **2001**, *56*, 293–303.
- [4] V. Hessel, H. Löwe, *Chem. Eng. Technol.* **2005**, *28*, 267–284.
- [5] A. J. deMello, *Nature* **2006**, *442*, 394–402.
- [6] K. Jähnisch, V. Hessel, H. Löwe, M. Baerns, *Angew. Chem.* **2004**, *116*, 410–451; *Angew. Chem., Int. Ed.* **2004**, *43*, 406–446.
- [7] K. F. Jensen, *MRS Bull.* **2006**, *2*, 101–107.
- [8] K. D. Nagy, B. Shen, T. F. Jamison, K. F. Jensen, *Org. Process Res. Dev.* **2012**, *16*, 976–981.
- [9] S. Mozharov, A. Nordon, D. Littlejohn, C. Wiles, P. Watts, P. Dallin, J. M. Girkin, *J. Am. Chem. Soc.* **2011**, *133*, 3601–3608.
- [10] V. Amarnath, D. C. Anthony, K. Amarnath, W. M. Valentine, L. A. Wetterau, D. G. Graham, *J. Org. Chem.* **1991**, *56*, 6924–6931.
- [11] B. Mothana, R. J. Boyd, *J. Mol. Struct.* **2007**, *811*, 97–107.
- [12] J. S. Moore, K. F. Jensen, *Org. Process Res. Dev.* **2012**, *16*, 1409–1415.
- [13] J. S. Moore, K. F. Jensen in *Microreactors in Organic Chemistry and Catalysis*, 2nd Ed., (Ed. T. Wirth), Wiley-VCH, **2013**, pp. 81–100.
- [14] DS Series Sampling Technology. Mettler Toledo, LLC. http://us.mt.com/us/en/home/products/L1_AutochemProducts/L2_in-situSpectroscopy/AgX-FiberConduit-Sampling-Technology-DS-Series.html, Accessed Nov. 7, 2010.
- [15] L. Knorr, *Ber. Dtsch. Chem. Ges.* **1885**, *18*, 299–311.
- [16] C. Paal, *Ber. Dtsch. Chem. Ges.* **1885**, *18*, 367–371.
- [17] J.-J. Li, E. J. Corey, Eds. *Name Reactions in Heterocyclic Chemistry*; John Wiley & Sons, Inc.: Hoboken, N. J., 2005.
- [18] V. Amarnath, K. Amarnath, W. M. Valentine, M. A. Eng, D. G. Graham, *Chem. Res. Toxicol.* **1995**, *8*, 234–238.
- [19] J. P. McMullen, K. F. Jensen, *Org. Process Res. Dev.* **2010**, *14*, 1169–1176.
- [20] J. P. McMullen, M. T. Stone, S. L. Buchwald, K. F. Jensen, *Angew. Chem.* **2010**, *122*, 7230–7234; *Angew. Chem., Int. Ed.* **2010**, *49*, 7076–7080.
- [21] J. P. McMullen, K. F. Jensen, *Org. Process Res. Dev.* **2011**, *15*, 398–407.
- [22] M. W. Bedore, N. Zaborenko, K. F. Jensen, T. F. Jamison, *Org. Process Res. Dev.* **2010**, *14*, 432–440.
-

(Kinetics in Flow)

Jason S. Moore and Klavs F. Jensen*
Page – Page

“Batch” Kinetics in Flow with Online IR
Analysis and Continuous Control



By continuously manipulating the flow rate and temperature, classical batch reactor time series data are obtained with microreactors under conditions of low dispersion with inline IR analysis. The approach requires significantly less time and materials compared to one-at-a-time flow experiments, allowing for the rapid generation of kinetic data.

Supporting Information

Section S1: Additional Figures

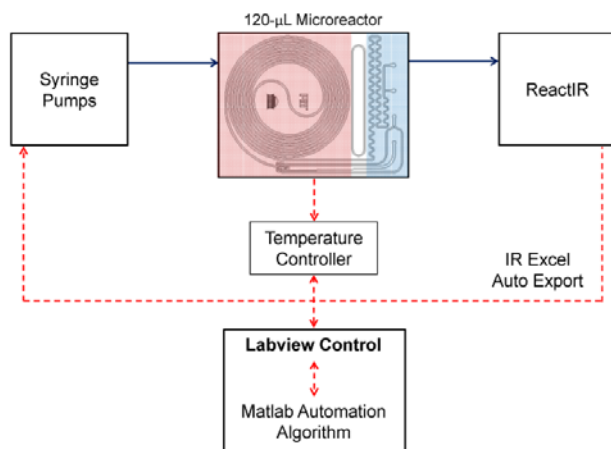


Figure S1. Automation system schematic. Solid lines represent fluid flow and dashed lines represent data flow.

An example of the resulting residence time profile for a residence time ramp experiment is given in Figure S2, which shows how the residence time is initially at τ_0 until time 0, at which point the residence time approaches the expected behavior from Eq. 3. The segment of the residence time that does not agree with Eq. 3 is due to the single reactor volume as the flow manipulation begins. Further description of this part of the residence time profile is provided in the following section.

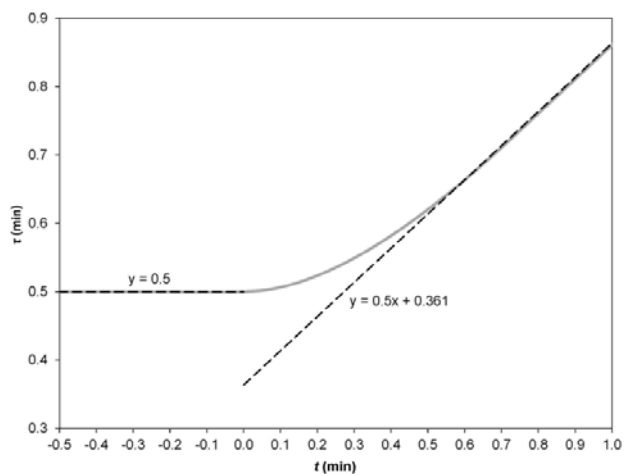


Figure S2. Example residence time, τ , vs. experiment time, t , with $\tau_0 = 0.5$ min, $S = 0.5$, and $\alpha = 0.693$. The gray line shows the residence time, τ , experienced by a fluid element.

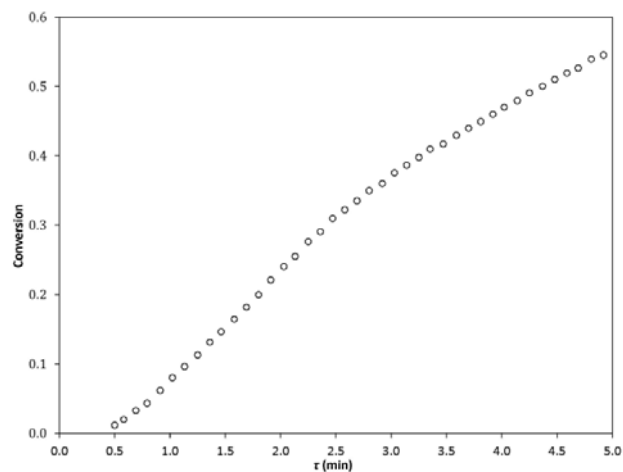


Figure S3. Conversion data collected from a residence time ramp experiment with $S = 0.5$ and an IR sample collection frequency of 15 seconds.

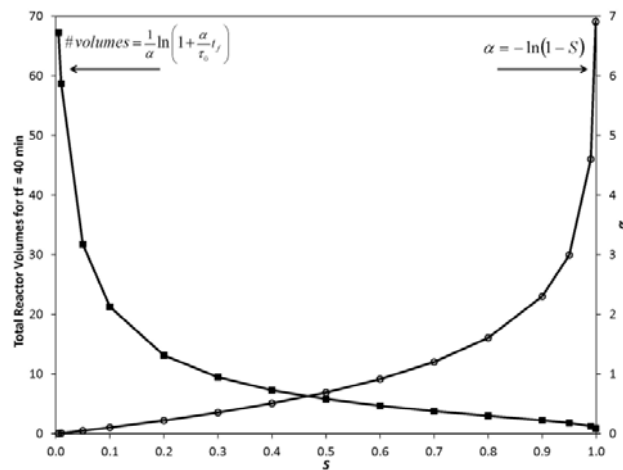


Figure S4. Reactor volumes for $t_f = 40$ min (■) and α (○), the rate of change of instantaneous residence time, as a function of slope, S .

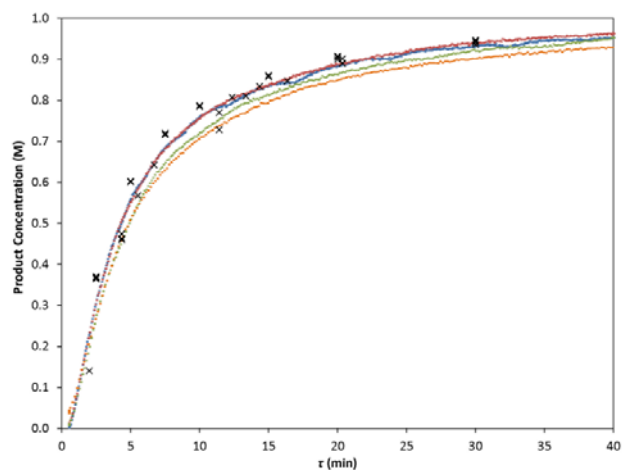


Figure S5. Residence time ramp results with $S = 1/4$ (blue), $S = 1/3$ (red), $S = 1/2$ (green), and $S = 2/3$ (orange). Steady states (\times).

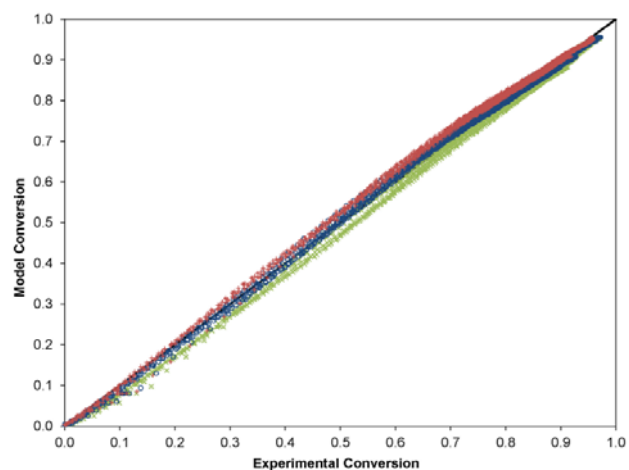


Figure S7. Comparison of model and experimental conversion for repeat 1 (\times), 2 (\circ), and 3 ($+$).

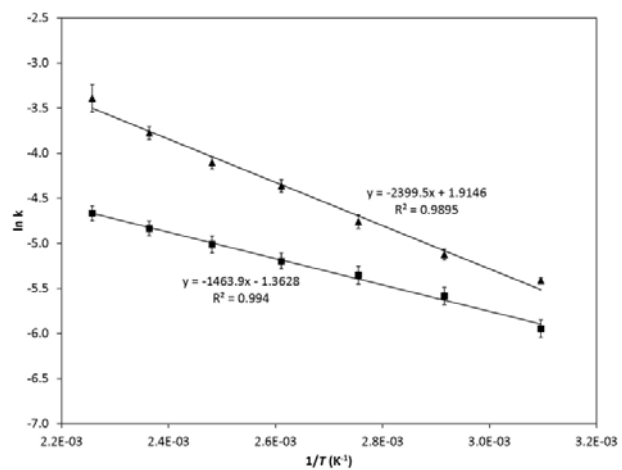


Figure S6. Arrhenius plot with $\ln k_1$ (square) and $\ln k_2$ (triangle).

Table S1. Arrhenius parameters. Errors given are standard error of the fit shown in Figure S6.

$\ln(k_1/(L/(mol \cdot s)))$	$E_{a,1}$ (kJ/mol)	$\ln(k_2/s^{-1})$	$E_{a,2}$ (kJ/mol)
-1.36 ± 0.14	12.2 ± 0.4	1.91 ± 0.29	20.0 ± 0.9

Section S2: Residence Time Derivations

Calculation of τ

Eq. 1 gives the instantaneous residence time, τ_{ins} , as a linear function of experiment time, t ,

$$\tau_{ins} = \tau_0 + \alpha t \quad (S1)$$

and the instantaneous flowrate, Q , through the reactor of volume V_r

$$Q(t) = \frac{V_r}{\tau_{ins}} \quad (S2)$$

Substituting in the definition of τ_{ins} from Eq. S1 into Eq. S2 yields the instantaneous flowrate as a function of experiment time:

$$Q(t) = \frac{V_r}{\tau_0 + \alpha t} \quad (S3)$$

The residence time, τ , of a fluid element entering the reactor at time t_i and exiting at time t_f is defined as

$$\tau = t_f - t_i \quad (S4)$$

Integrating for the fluid element residence time as it travels through the reactor volume:

$$V_r = \int_{t_i}^{t_f} Q(t) dt = \int_{t_i}^{t_f} \frac{V_r}{\tau_0 + \alpha t} dt \quad (S5)$$

Dividing Eq. S5 through by V_r :

$$1 = \frac{1}{\alpha} \ln(\tau_0 + \alpha t) \Big|_{t_i}^{t_f} \quad (S6)$$

Multiplying Eq. S6 through by α and substituting in the time bounds:

$$\alpha = \ln\left(\frac{\tau_0 + \alpha t_f}{\tau_0 + \alpha t_i}\right) \quad (S7)$$

Exponentiating Eq. S7 and multiplying through by the logarithm denominator:

$$e^\alpha (\tau_0 + \alpha t_i) = \tau_0 + \alpha t_f \quad (S8)$$

Solving Eq. S8 for t_i as function of t_f :

$$t_i = e^{-\alpha} t_f - \left(1 - e^{-\alpha}\right) \frac{\tau_0}{\alpha} \quad (S9)$$

Substitution for τ

Substituting Eq. S9 into Eq. S4 yields the fluid element residence time, τ , as a function of t_f :

$$\tau = t_f - \left(e^{-\alpha} t_f - \left(1 - e^{-\alpha}\right) \frac{\tau_0}{\alpha} \right) \quad (S10)$$

Rearranging Eq. S10:

$$\tau = \left(1 - e^{-\alpha}\right) \left(t_f + \frac{\tau_0}{\alpha} \right) \quad (S11)$$

Defining the variable S as the slope between t_f and τ , as in Eq. 4:

$$S = \left(1 - e^{-\alpha}\right) \quad (S12)$$

Substituting S into Eq. S11 gives the linear relationship between τ and t_f that is used for Figure S5:

$$\tau = \frac{S}{\alpha} \tau_0 + S t_f \quad (S13)$$

Corrected τ

However, as noted in the main text, measurement occurs at t_m after the fluid has flowed a volume V_d from the reactor outlet. This volume can be treated in the same way as the reactor volume in Eq. S5 to find the necessary time corrections:

$$V_d = \int_{t_f}^{t_m} \frac{V_r}{\tau_0 + \alpha t} dt \quad (S14)$$

Solving the integral and dividing Eq. S14 by V_r :

$$\frac{V_d}{V_r} \alpha = \ln\left(\frac{\tau_0 + \alpha t_m}{\tau_0 + \alpha t_f}\right) \quad (S15)$$

Exponentiating Eq. S15 and multiplying through by the logarithm denominator:

$$e^{\frac{V_d}{V_r} \alpha} (\tau_0 + \alpha t_f) = \tau_0 + \alpha t_m \quad (S16)$$

Solving Eq. S16 for t_m as a function of t_f :

$$t_m = e^{\frac{V_d}{V_r} \alpha} t_f + \left(e^{\frac{V_d}{V_r} \alpha} - 1 \right) \frac{\tau_0}{\alpha} \quad (S17)$$

Solving Eq. S17 for t_f as a function of t_m :

$$t_f = e^{-\frac{V_d}{V_r} \alpha} t_m - \left(1 - e^{-\frac{V_d}{V_r} \alpha} \right) \frac{\tau_0}{\alpha} \quad (S18)$$

Eq. S13 can be rearranged for t_f as function of τ :

$$t_f = \frac{e^\alpha}{e^\alpha - 1} \tau - \frac{\tau_0}{\alpha} \quad (S19)$$

which can be substituting into Eq. S18:

$$\frac{e^\alpha}{e^\alpha - 1} \tau - \frac{\tau_0}{\alpha} = e^{-\frac{V_d}{V_r} \alpha} t_m - \left(1 - e^{-\frac{V_d}{V_r} \alpha} \right) \frac{\tau_0}{\alpha} \quad (S20)$$

Solving Eq. S20 for τ as a function of measurement time, t_m , yields

$$\tau = \left(1 - e^{-\alpha}\right) e^{\frac{V_d}{V_r} \alpha} \left(t_m + \frac{\tau_0}{\alpha} \right) \quad (S21)$$

which is used in Figure 2.

If $t_i < 0$ and $t_f \geq 0$

As shown by Figure S2, the reactor volume during initiation of the residence time ramp undergoes a residence time profile that can be found by solving

$$V_r = \int_{t_i}^0 \frac{V_r}{\tau_0} dt + \int_0^{t_f} \frac{V_r}{\tau_0 + \alpha t} dt \quad (S22)$$

where the first integral is for t_i previous to time 0. Solving the integrals and dividing by V_r :

$$1 = \frac{-t_i}{\tau_0} + \frac{1}{\alpha} \ln\left(\frac{\tau_0 + \alpha t_f}{\tau_0}\right) \quad (S23)$$

Solving Eq. S23 for t_i :

$$t_i = \tau_0 \left(\frac{1}{\alpha} \ln\left(\frac{\tau_0 + \alpha t_f}{\tau_0}\right) - 1 \right) \quad (S24)$$

Substituting in Eq. S4 into Eq. S24 and solving for τ :

$$\tau = t_f - \tau_0 \left(\frac{1}{\alpha} \ln\left(\frac{\tau_0 + \alpha t_f}{\tau_0}\right) - 1 \right) \quad (S25)$$

